This article was downloaded by: [Tomsk State University of Control Systems and Radio]
On: 23 February 2013, At: 03:12
Publisher: Taylor & Francis
Informa Ltd Registered in England and Wales Registered Number: 1072954 Registered office: Mortimer House, 37-41 Mortimer Street, London W1T 3JH, UK

Molecular Crystals and Liquid Crystals
Publication details, including instructions for authors and subscription information:
http://www.tandfonline.com/loi/gmcl16

Effects of Molecular Length on Nematic Mixtures

J. David Margerum [a], Siu-May Wong [a], Anna M. Lackner [a] & John E. Jensen [a]
[a] Hughes Research Laboratories, 3011 Malibu Canyon Road, Malibu, California, 90265, U.S.A.
Version of record first published: 14 Oct 2011.

To cite this article: J. David Margerum , Siu-May Wong , Anna M. Lackner & John E. Jensen (1981): Effects of Molecular Length on Nematic Mixtures, Molecular Crystals and Liquid Crystals, 68:1, 157-174

To link to this article: http://dx.doi.org/10.1080/00268948108073561

PLEASE SCROLL DOWN FOR ARTICLE

Full terms and conditions of use: http://www.tandfonline.com/page/terms-and-conditions

This article may be used for research, teaching, and private study purposes. Any substantial or systematic reproduction, redistribution, reselling, loan, sub-licensing, systematic supply, or distribution in any form to anyone is expressly forbidden.

The publisher does not give any warranty express or implied or make any representation that the contents will be complete or accurate or up to date. The accuracy of any instructions, formulae, and drug doses should be independently verified with primary sources. The publisher shall not be liable for any loss, actions, claims, proceedings, demand, or

costs or damages whatsoever or howsoever caused arising directly or indirectly in connection with or arising out of the use of this material.

Downloaded by [Tomsk State University of Control Systems and Radio] at 03:12 23 February 2013

Mol. Cryst. Liq. Cryst., 1981, Vol. 68, pp. 157–174
0026-8941/81/6801-0157 $06.50/0
© 1981 Gordon and Breach, Science Publishers, Inc.
Printed in the United States of America

Downloaded by [Tomsk State University of Control Systems and Radio] at 03:12 23 February 2013

Effects of Molecular Length on Nematic Mixtures

II Anisotropic and Dynamic Scattering Properties of 4-Alkoxyphenyl 4-Alkylcyclohexanecarboxylate Mixtures†

J. DAVID MARGERUM, SIU-MAY WONG, ANNA M. LACKNER, and JOHN E. JENSEN

Hughes Research Laboratories, 3011 Malibu Canyon Road, Malibu, California 90265, U.S.A.

(*Received August 11, 1980*)

The properties of nematic liquid-crystal mixtures of 4-alkoxyphenyl *trans*-4-alkylcyclohexanecarboxylates are studied as a function of temperature and their average molecular length ($\bar{L}$). Mixtures are prepared with clearpoints near 72°C (±3°C) and with $\bar{L}$ varying between 21.20 and 26.15 Å. At 25°C, their flow viscosity increases exponentially (from 16.3 to 50.6 cP) as $\bar{L}$ increases. The conductivity anisotropy ($\sigma_{\parallel}/\sigma_{\perp}$) also varies tremendously, decreasing from 1.62 to 0.49 as $\bar{L}$ increases, when compared at 25°C with tetrabutylammonium tetraphenylboride as dopant. The low values of $\sigma_{\parallel}/\sigma_{\perp}$ and its temperature dependence indicate that cybotatic nematic characteristics occur when the average total number of alkyl carbons from both end groups is 8.5 or more. Short range smectic effects are dominant in the longer mixtures. All of the mixtures have a negative dielectric anisotropy, which linearly becomes less negative with increasing $\bar{L}$. At 25°C, dynamic scattering (DS) is observed only in the shorter $\bar{L}$ mixtures (where $\sigma_{\parallel}/\sigma_{\perp} > 1$), and the DS decay times are relatively fast. Comparisons are made with similar studies on *p*-alkoxyphenyl *p*-alkylbenzoate mixtures.

INTRODUCTION

In recent years, there has been considerable interest regarding the incorporation of cyclohexane structures into liquid-crystal (LC) compounds and mixtures.[1-6] Most of the studies have been on materials with positive dielectric anisotropy, such as 4-cyanophenylcyclohexanes, for use in twisted nematic displays based on polarization switching.[2-6] These cyanophenylcyclohexanes have a lower viscosity and birefringence than do the corresponding cyanobi-

†Presented at the 8th International Liquid Crystal Conference, Kyoto, Japan, July 1980.

phenyl nematic liquid crystals. Esters with phenyl cyclohexanecarboxylate structures have been reported to have wide nematic temperature ranges,[1] but relatively little has been reported on their anisotropic and electrooptical properties. We are interested in the use of cyclohexanecarboxylate esters as nematic mixtures for both dc- and ac-activated dynamic-scattering (DS) displays, particularly to obtain wide temperature range mixtures with fast response times. Since we have found that the average molecular length ($\bar{L}$) of *p*-alkoxylphenyl *p*-alkylbenzoate mixtures has a large effect on their nematic properties,[7] the present study is directed particularly at the effects of molecular length on the properties of mixtures 4-alkoxylphenyl *trans*-4-alkylcyclohexanecarboxylates. We are especially interested in the effect of $\bar{L}$ on the viscosity, dielectric anisotropy, conductivity anisotropy, and DS response of these mixtures, and in comparing these results with those from the similar phenyl benzoate mixtures.

EXPERIMENTAL

The cyclohexane liquid-crystal compounds were prepared by reacting the appropriate 4-alkoxyphenol with a 4-alkylcyclohexanecarbonyl chloride. The latter are obtained by first carrying out a catalytic reduction (H_2/ Rh in a Paar apparatus) of the *p*-alkylbenzoic acid and then treating it with thionyl chloride. The catalytic reduction gives the *cis*-4-alkylcyclohexanecarboxylic acid, but heating the acid chloride converts it largely to the *trans*-4-alkylcyclohexanecarbonyl chloride. The mixture of these *cis* and *trans* acid chlorides are esterified, and the lower melting *cis* ester is removed from the 4-alkoxyphenyl *trans*-4-alkylcyclohexanecarboxylate by recrystallizations. Purity is checked by thin-layer chromatography and by high-pressure liquid chromatography (Waters Assoc. Model ALC-202/401, with a microporasil column). We estimate that there is less than 1% impurity in each ester. Thermal analysis data on the melting point (mp), clearpoint (clpt), and heat of fusion (ΔH_f) are obtained by differential scanning calorimetry (DSC) using a Mettler TA2000B thermal analysis system.

Our other experimental techniques are essentially the same as in paper I of this series.[7] The density is measured in calibrated pycnometer tubes, as a function of temperature. The flow viscosity (η) is measured in calibrated Cannon-Manning-type viscometer tubes held in a temperature-controlled bath. The calibrated ranges were 3 to 15, 7 to 35, and 20 to 100 cS, respectively, in three different size tubes. Overlapping results from different tubes are in good agreement (i.e., there is no tube size effect on η). The refractive indices are measured with a Leitz-Jelly micro-refractometer at 589 nm. The dielectric anisotropy and conductivity anisotropy are measured as described previously,[7,8] using 503-μm-thick cells in a 7-kG magnetic field. The samples are

Downloaded by [Tomsk State University of Control Systems and Radio] at 03:12 23 February 2013

Downloaded by [Tomsk State University of Control Systems and Radio] at 03:12 23 February 2013

doped with tetrabutylammonium tetraphenylboride (TBATPB) or tetrabutylammonium trifluoromethanesulfonate (TBATMS) by adding 0.1% of the salt, warming to dissolve, cooling at room temperature for 12 hr, and filtering through a 0.2-μm filter. The DS measurements are made in transmission with unpolarized green light using glass cells with indium tin oxide (ITO) transparent electrodes. Threshold voltages are made at 30, 20, and 10 Hz, in cells with nominal spacers of 25.4 μm, using baked polyvinyl alcohol (PVA) coatings rubbed for surface-|| alignment, and using an 800-Å coating of sputter-deposited SiO_2 treated with $C_{22}H_{45}OH$ for surface-$\perp$-alignment.[9] The DS decay times are measured from 10% to 90%T at 25° C using SiO_2-overcoated ITO electrodes on 12.7-mm-thick optical flats with SiO_x pad spacers. The surface-|| cell (15.43-μm-thick spacing) has a rubbed PVA coating, while the surface-$\perp$ cell (15.86 μm) is treated with $C_{18}H_{37}OH$. Undoped samples are used for the dielectric field effect transition threshold voltage at 1 kHz in surface-$\perp$ cells.

RESULTS AND DISCUSSION

LC components and mixtures

The thermal properties for the six nematic compounds used in these studies are shown in Table I, where R and R' are the n-alkyl groups in the general structure shown in Figure 1a. Our observed melting points and clearpoints are higher than the literature values, indicating that our compounds are of higher purity. We did not observe the low melting point of smectic-to-nematic transition reported for 60–(C)5. Mixtures were prepared with the compositions shown in Table II. These were primarily mixtures from calculated eutectic compositions that were chosen to be room-temperature nematics, to have similar clearpoint temperatures, and to have as wide a range of $\bar{L}$ as possible. The

TABLE I

Thermal properties of phenyl cyclohexanecarboxylates

Compound			mp, °C		clpt, °C		ΔH_f
Code	RO	R'	Obs.	Lit.[a]	Obs.	Lit.[a]	kcal/mole
10–(C)5	CH_3O	n-C_5H_{11}	40.9	36	71.3	63.5	5.01
20–(C)3	C_2H_5O	n-C_3H_7	49.0	47	79.8	78.5	6.60
20–(C)5	C_2H_5O	n-C_5H_{11}	56.9	55	85.9	85.5	7.69
40–(C)4	n-C_4H_9O	n-C_4H_9	40.5	38	70.0	68.5	4.12
60–(C)4	n-$C_6H_{13}O$	n-C_4H_9	26	25	70.0	69.0	5.36
60–(C)5	n-$C_6H_{13}O$	n-C_5H_{11}	32.2[b]	24(38.5)[b]	79.8	78.5	5.06

[a] D. Demus, H.-J. Deutscher, F. Kuschel, H. Schubert, Offenlegungsschrift 2429093, Bundesrepublik Deutschland, Deutches Patentant, (Jan. 23, 1975).

[b] Smectic to nematic transition reported at 38.5°C, but not obs. here.

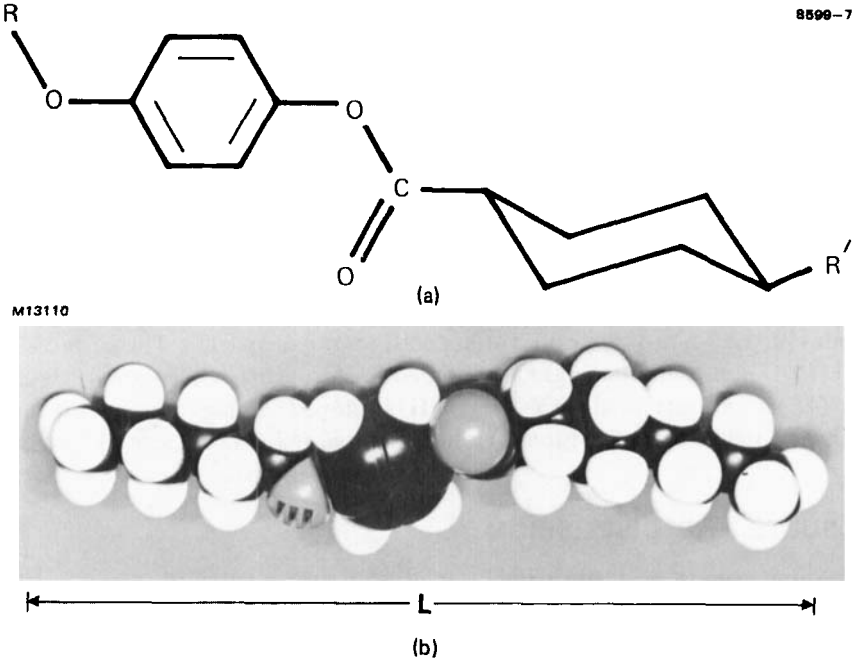

FIGURE 1 (a) General structure of mixture components. (b) Model of 4-hexyloxyphenyl 4-butylcyclohexanecarboxylate, or 60-(C)4, showing the molecular length (L = 26.15 Å) used.

results in Table III show a close correlation between the calculated and the observed nematic ranges of these mixtures. The resistivities of the undoped mixtures are greater than $10^{12}\Omega$-cm. The molecular length (L) of each compound is measured from the end-to-end distance in CPK models, as indicated in Figure 1b. The average length, $\bar{L}$, of a mixture is obtained by summing the product of the mole fraction and the L of each component.

TABLE II

Composition of liquid-crystal mixtures

Compound		Mole fraction in mixtures						
Code	Length, L, Å	A	B	C	D	E	F	G
10-(C)5	21.40	0.497	0.463	0.394	0.283	—	—	—
20-(C)3	20.06	0.311	—	—	—	—	—	—
20-(C)5	22.53	0.192	—	0.135	—	—	—	—
40-(C)4	23.84	—	0.537	0.470	0.358	0.507	0.483	—
60-(C)4	26.15	—	—	—	—	—	—	1.000
60-(C)5	27.41	—	—	—	0.359	0.493	0.517	—
HRL mixture No.		6N7	6N4	6N5	6N10	6N6	6N6R	60-(C)4

Downloaded by [Tomsk State University of Control Systems and Radio] at 03:12 23 February 2013

TABLE III

Average length and nematic range of mixtures

Mixture	$\bar{L}$, average length, Å	No. R + R' carbons	mp °C		clpt, °C	
			Calc.[a]	Obs.	Calc.[a]	Obs.
A	21.20	5.88	16.2	14.4	76.7	76.1
B	22.71	7.07	13.9	14.2	70.6	69.3
C	22.70	7.07	8.8	4.8	72.6	71.6
D	24.43	8.51	−1.1	−10.0	73.8	73.2
E	25.60	9.48	—	13.4	—	75.4
F	25.68	9.55	9.9	—	75.0	74.8
G	26.15	10.00	—	26.00	—	70.0

[a] Calculated eutectic mixture, using Schroeder–Van Laar equation.

Refractive index, birefringence, density, and dielectric constant

Plots of refractive indices ($n_{\parallel}$ and $n_{\perp}$), birefringence (Δn), density (d), and dielectric constant ($\epsilon_{\perp}$) of the mixtures are shown in Figure 2 as a function of their $\bar{L}$. Both $n_{\parallel}$ and $n_{\perp}$ decrease slightly as $\bar{L}$ increases, as expected since longer $\bar{L}$ increases just the aliphatic end group length of similar molecules already containing a cyclohexane ring in the central group. Their birefringence is small and is nearly independent of $\bar{L}$, with $\Delta n = 0.085 \pm 0.003$ at room temperature. This is substantially smaller than the birefringence of similar phenyl benzoate esters, in which Δn varied between 0.153 and 0.134 over the same $\bar{L}$ range.[7] The $n_{\perp}$ of these cyclohexane ester mixtures is also lower than that of comparable length phenyl benzoate mixtures. The d and $\epsilon_{\perp}$ values decrease approximately linearly as $\bar{L}$ increase. Both the magnitudes of d and $\epsilon_{\perp}$ and their rates of decrease with $\bar{L}$ are smaller in these mixtures than in the phenyl benzoate series, as expected since the central group contains a cyclohexane ring in place of a phenyl group.

Flow viscosity

The flow viscosities of these mixtures are shown as a function of temperature in Figure 3. Note that the plot for G includes a point above the clearpoint where η increases. In each mixture, the plots of log η versus T^{-1} deviate from the linear relationship often found for liquids and LCs. The effect of $\bar{L}$ on the flow viscosity at a given temperature is quite large, as shown in Figure 4. At 25° C, the viscosity increases exponentially with increasing molecular length. This rapid increase of η with $\bar{L}$ is probably related to the strong cybotactic nematic character observed (described below) for these mixtures as their $\bar{L}$ increases. At 25° C, the short length *RO*-(C)*R'* mixtures have lower η's than do the corresponding length *RO*-*R'* (phenylbenzoate) mixtures (e.g., 16 and 34

Downloaded by [Tomsk State University of Control Systems and Radio] at 03:12 23 February 2013

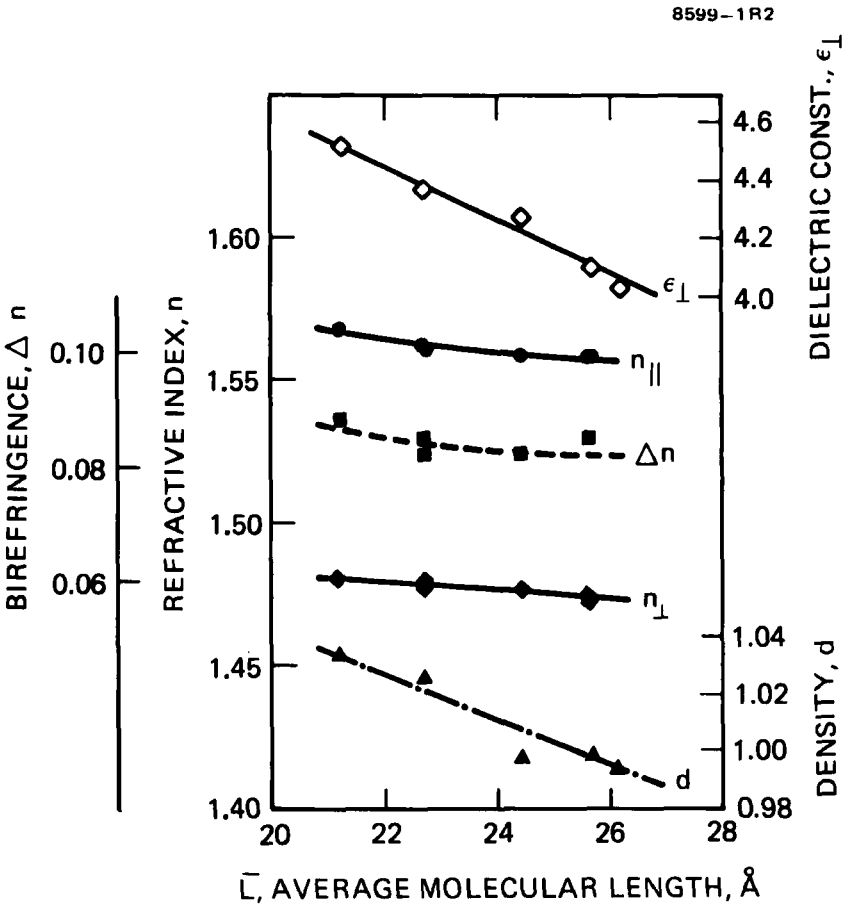

FIGURE 2 Refractive indices, birefringence, density, and dielectric constant of *RO*-(C)*R'* mixtures as a function of $\bar{L}$. (Δn at 22.8°C, d and $\epsilon_\perp$ at 25.0°C.)

cP, respectively, at $\bar{L} = 21$ Å). However, the longer length *RO*-(C)*R'* mixtures have higher η's than do the *RO*-*R'* mixtures (e.g., 48 and 41 cP, respectively, at $\bar{L} = 26$ Å). Thus, the substitution of cyclohexane rings for benzene rings in LC components does not always give a lower viscosity nematic mixture; it does so only for the short length ester mixtures in this series.

Conductivity anisotropy

The conductivity anisotropy ($\sigma_\parallel / \sigma_\perp$) of five of the mixtures is shown in Figure 5 as a function of temperature. Although the solubility and conductivity of TBATPB in a mixture decrease as $\bar{L}$ increases, our experience indicates that this should have no significant effect on the anisotropy measurements.[7,8,10]

Downloaded by [Tomsk State University of Control Systems and Radio] at 03:12 23 February 2013

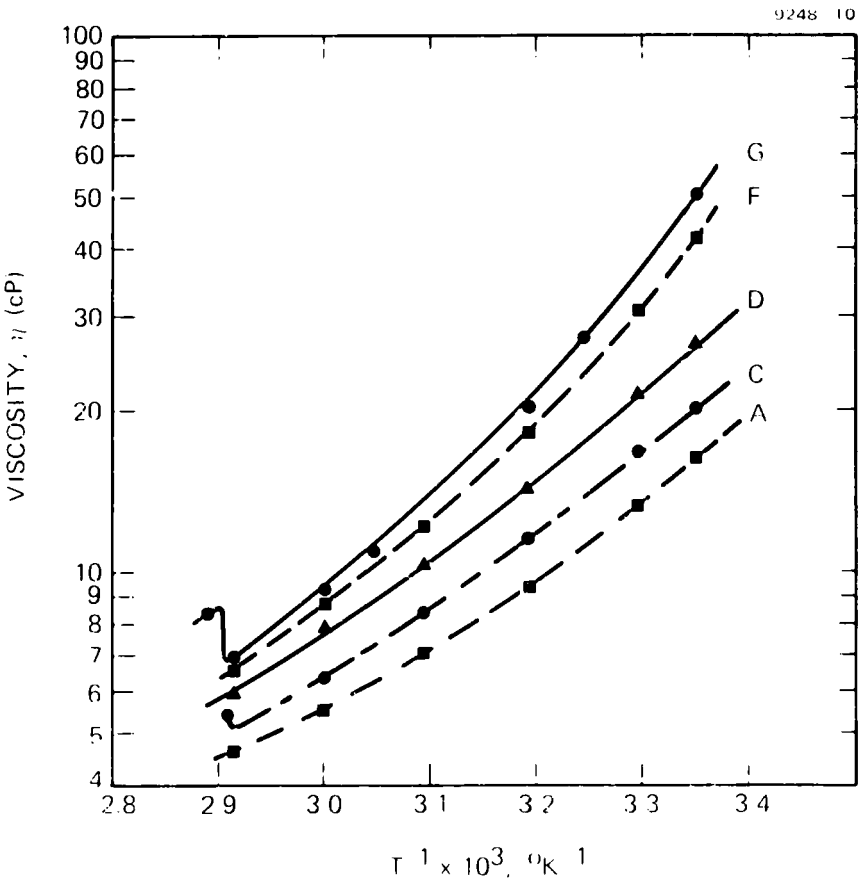

FIGURE 3 Effect of temperature on flow viscosity of *RO*-(C)*R'* mixtures.

The $\sigma_{\|}/\sigma_{\perp}$ values in A, the shortest L̄ mixture, are high (1.61 to 25° C) and decrease with increasing temperature, as is characteristic of a nematic liquid crystal. The values in C, a slightly longer length mixture, are not quite as high as in mixture A and are nearly constant over a wide temperature range. The $\sigma_{\|}/\sigma_{\perp}$ values in D increase as the temperature increases, which is taken as evidence for some cybotactic character[11-14] (short range smetic order) at temperatures below about 50° C. Mixture E and compound G have the longest L̄'s, and their $\sigma_{\|}/\sigma_{\perp}$ values are considerably below 1.0, which is characteristic of a smectic LC or very strongly cybotactic nematic LC. From the curves in Figure 5, we conclude that *RO*-(C)*R'* mixtures with an average of 8.5 or more $R + R'$ alkyl carbons have cybotactic nematic characteristics. The corresponding number of $R + R'$ carbons for cybotactic effects in the *RO*-*R'* mixtures is 10 carbons or more.[7] Thus, the presence of a cyclohexanecarboxylate

Downloaded by [Tomsk State University of Control Systems and Radio] at 03:12 23 February 2013

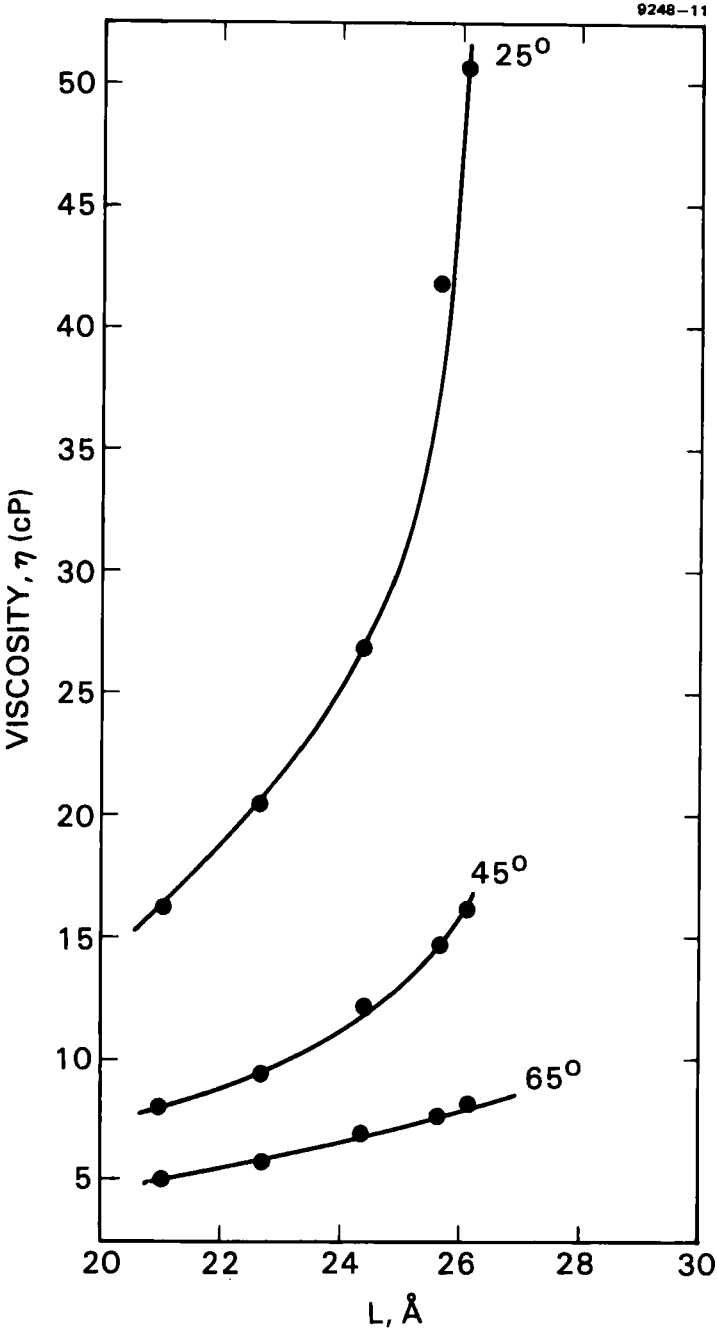

FIGURE 4 Effect of L on viscosity of *RO*-(C)*R'* mixtures.

Downloaded by [Tomsk State University of Control Systems and Radio] at 03:12 23 February 2013

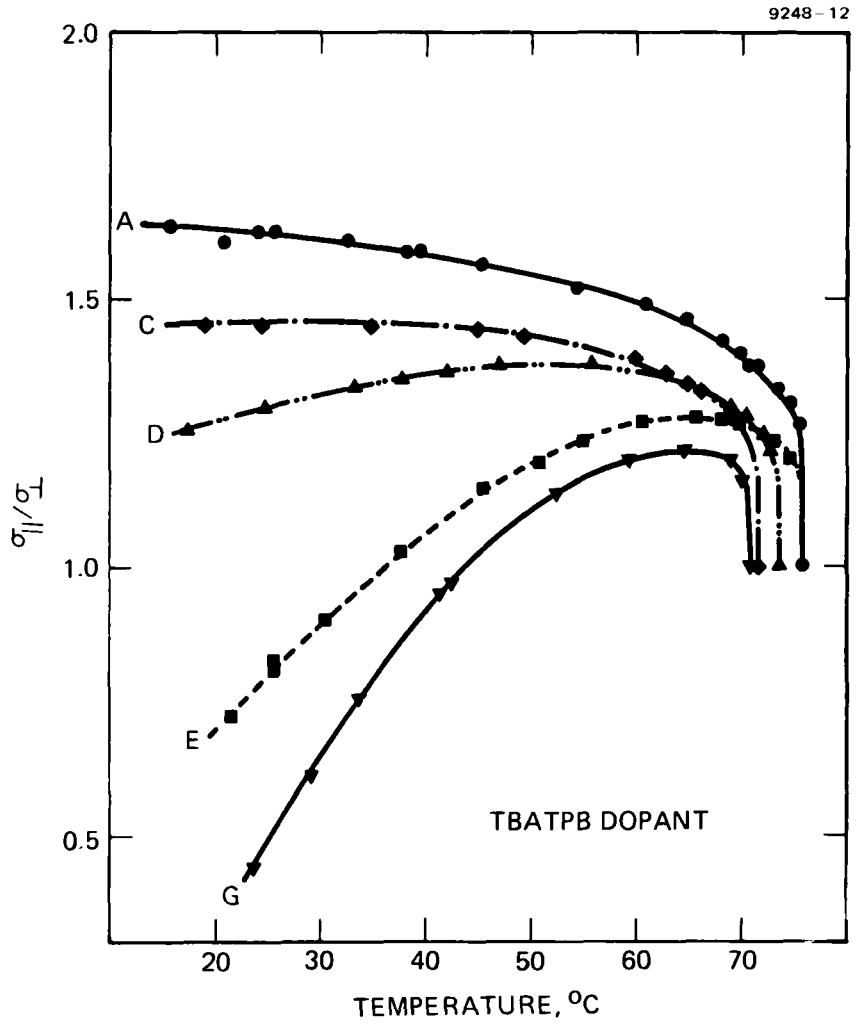

FIGURE 5 Conductivity anisotropy of TBATPB in *RO*-(C)*R'* mixtures as a function of temperature.

group in place of a benzoate group reduces the average length at which cybotactic effects are observed in their alkoxyphenyl ester LCs.

Because of the limited solubility of TBATPB in these cyclohexane esters, we also studied TBATMS, which is a smaller, more polar salt. It is more soluble and provides adequate conductivity for DS studies. Since we have previously found[8,10] that the $\sigma_{\parallel}/\sigma_{\perp}$ values for TBATMS at a given temperature increase at low resistivity, we kept the $\rho_{\perp}$ (25°) of these samples in the range of 8.4×10^8 to 5.8×10^9 Ω-cm. The results are shown in Figure 6. The cybotac-

Downloaded by [Tomsk State University of Control Systems and Radio] at 03:12 23 February 2013

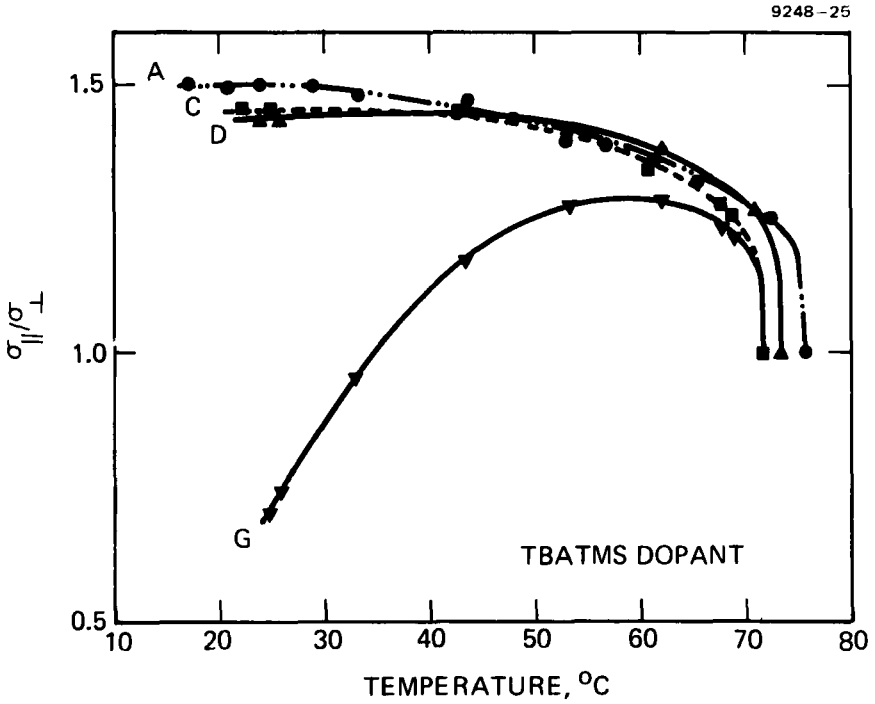

FIGURE 6 Conductivity anisotropy of TBATMS in *RO*-(C)*R'* mixtures as a function of temperature.

tic nematic criterion ($\sigma_{\parallel}/\sigma_{\perp}$ increasing with temperature) is less pronounced with TBATMS than with TBATPB, especially in mixture D. In other nematic LCs, we have found that at room temperature the $\sigma_{\parallel}/\sigma_{\perp}$ of TBATMS was less than that of TBATPB, as is the case in mixture A. However, they are about the same in mixture C, and TBATMS has higher $\sigma_{\parallel}/\sigma_{\perp}$ values than TBATPB in mixtures D and G. This is seen more clearly in Figure 7, where the values are compared at two reduced temperatures. (In these mixtures, the reduced temperatures of 0.86 and 0.96 correspond to an average of about 26 and 60° C, respectively.) At $T/T_c = 0.86$, the curves for the two dopants cross because the values for TBATPB decrease more rapidly than those for TBATMS as $\bar{L}$ increases. However, at the higher reduced temperature of 0.96, the $\sigma_{\parallel}/\sigma_{\perp}$ values for TBATMS are less than those of TBATPB throughout the $\bar{L}$ range. The cybotactic nematic character of the *RO*-(C)*R'* mixtures clearly has a larger effect on the conductivity anisotropy of the TBATPB dopant than of the TBATMS dopant. In Figure 7, both plots of $\sigma_{\parallel}/\sigma_{\perp}$ versus $\bar{L}$ at $T/T_c = 0.86$ show a large deviation from linearity due to the strong cybotactic nematic ordering in the longer $\bar{L}$ mixtures.

Downloaded by [Tomsk State University of Control Systems and Radio] at 03:12 23 February 2013

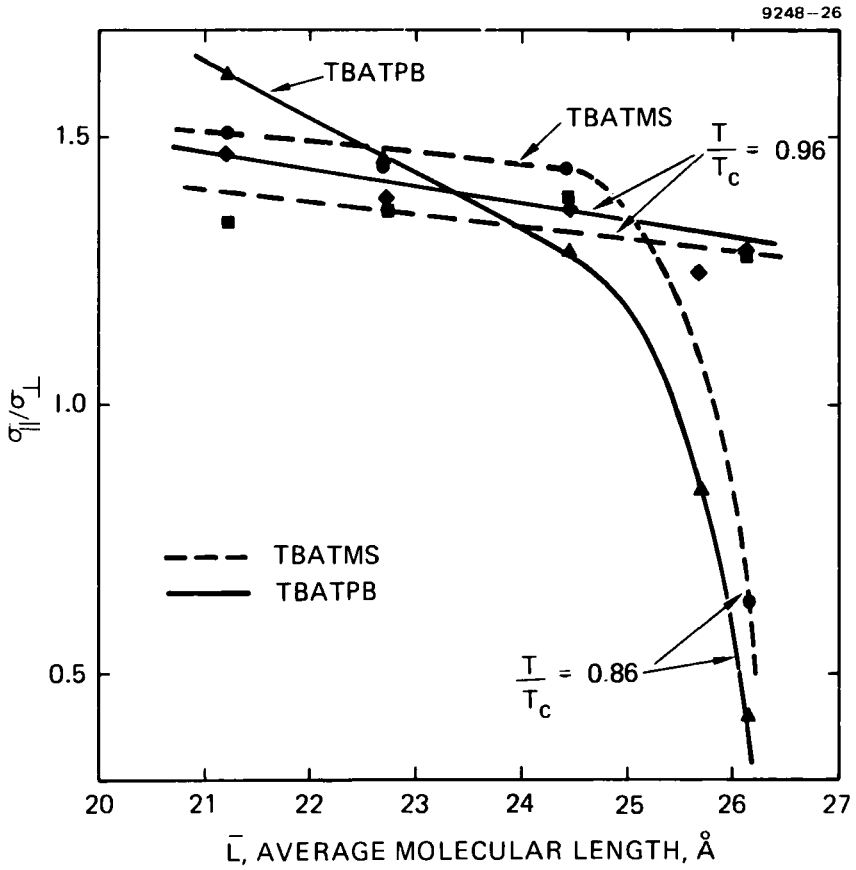

FIGURE 7 Effect of $\bar{L}$ on conductivity anisotropy of *RO*-(C)*R'* mixtures at reduced temperatures. (T = measurement temperature and T_c = clearpoint, both in °K).

Dielectric anisotropy

The effects of temperature on the dielectric constants of these mixtures are shown in Figure 8. Because $\epsilon_\perp$ decreases appreciably while $\epsilon_\parallel$ changes only slightly with increasing temperature, the values of $-\Delta\epsilon$ decrease linearly as temperature increases in the 20 to 60° C range. This effect of temperature on $\Delta\epsilon$ is the one we would expect in the absence of molecular associations. Thus, while $\sigma_\parallel/\sigma_\perp$ and viscosity effects show strong evidence for cybotactic nematic molecular order, the $\Delta\epsilon$ effects do not indicate any molecular pairing of polar groups. (In contrast, the longer $\bar{L}$ *RO-R'* mixtures[7] showed less cybotactic nematic association than these *RO*-(C)*R'* mixtures, while the shorter $\bar{L}$ *RO-R'* mixtures showed evidence of polar associations—as inferred by their $-\Delta\epsilon$ values going through a maximum as temperature increased.) These

Downloaded by [Tomsk State University of Control Systems and Radio] at 03:12 23 February 2013

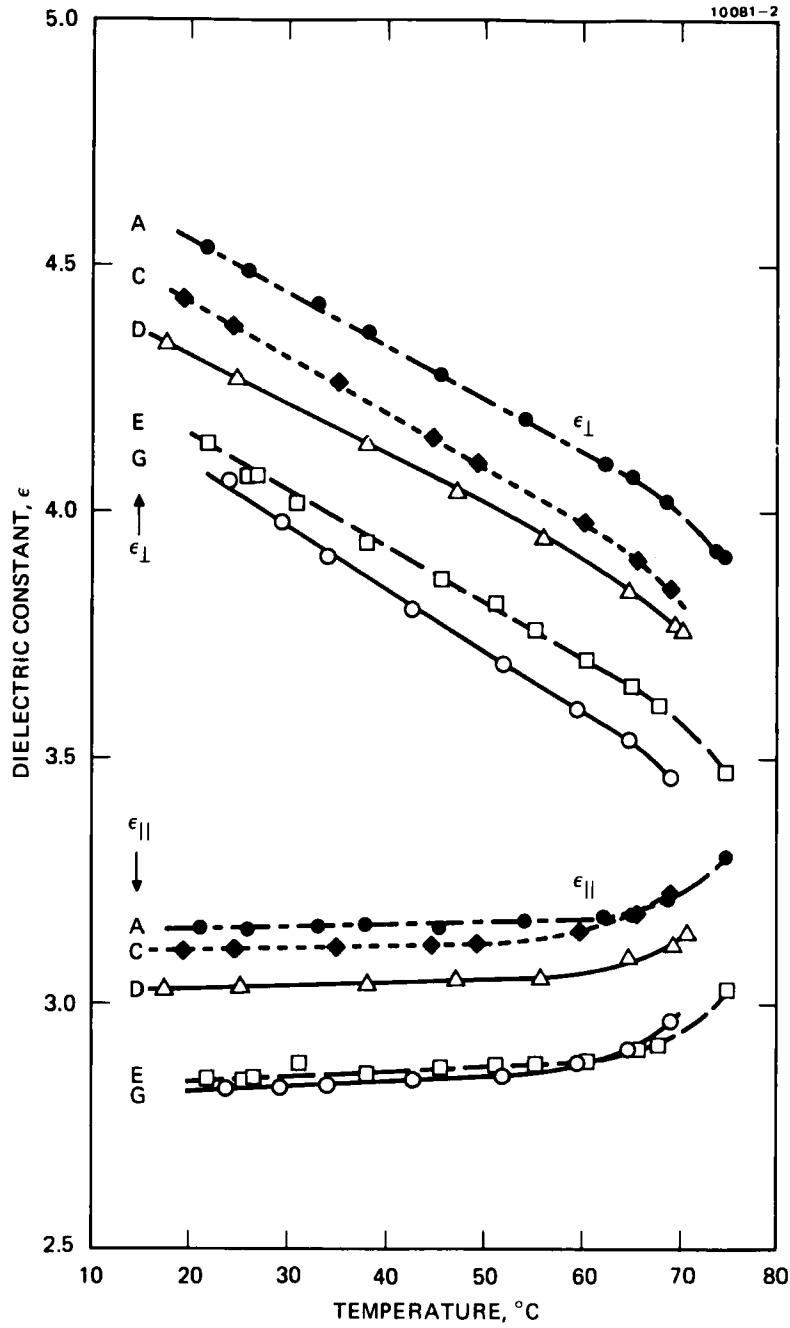

FIGURE 8 Dielectric constants of *RO*-(C)*R'* mixtures as a function of temperature (5 kHz).

Downloaded by [Tomsk State University of Control Systems and Radio] at 03:12 23 February 2013

mixtures have much more negative $\Delta\epsilon$ values (between -1.34 and -1.20 at 25° C) than do the corresponding *RO–R′* mixtures. As shown in Figure 9, $-\Delta\epsilon$ at a given reduced temperature decreases linearly with increasing $\bar{L}$. (In the *RO–R′* mixtures, $-\Delta\epsilon$ increased with $\bar{L}$.) The nearly parallel changes of $-\Delta\epsilon$ with temperature (Figure 8) and with $\bar{L}$ (Figure 9) indicate that the dielectric effects in these *RO*-(C)*R′* mixtures are not significantly affected by the large differences in viscosity and cybotactic nematic character.

Field effect transition and elastic constant

The threshold voltage for the field-effect realignment, $(V'_{th})_{FE}$, of these undoped LC mixtures is shown by the lower line in Figure 10. It is nearly unchanged by the changes in $\bar{L}$. The corresponding k_{33} (bend elastic constant) values also do not vary much with $\bar{L}$, as shown in Table IV.

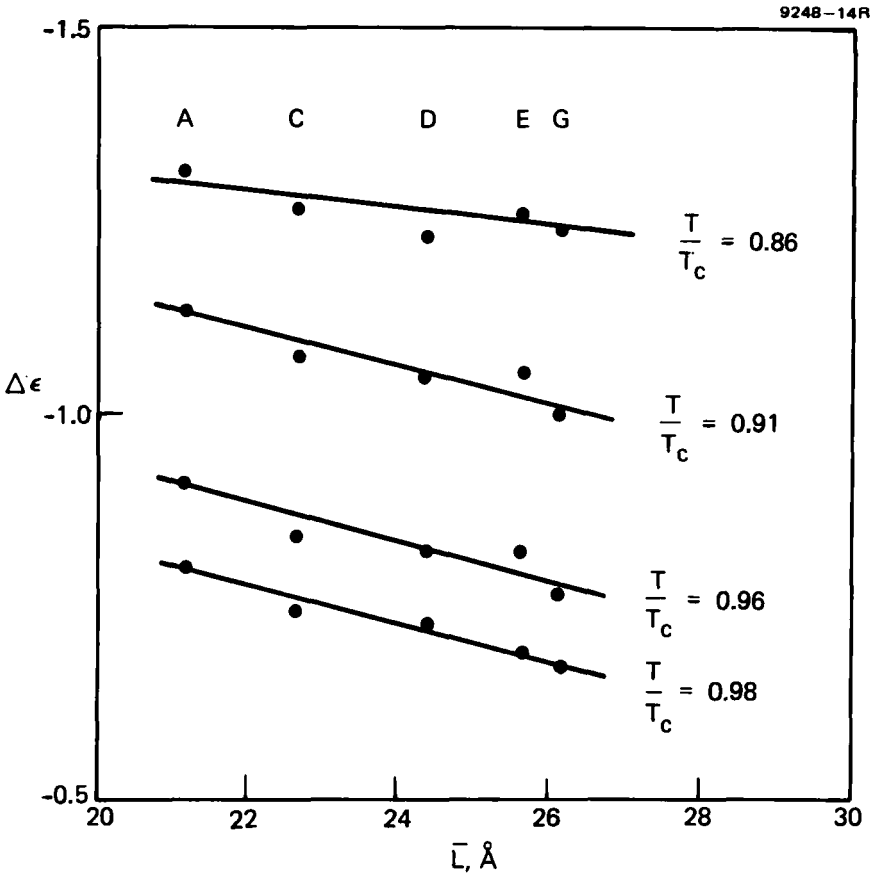

FIGURE 9 Effect of $\bar{L}$ on dielectric anisotropy of *RO*-(C)*R′* mixtures at four reduced temperatures.

Downloaded by [Tomsk State University of Control Systems and Radio] at 03:12 23 February 2013

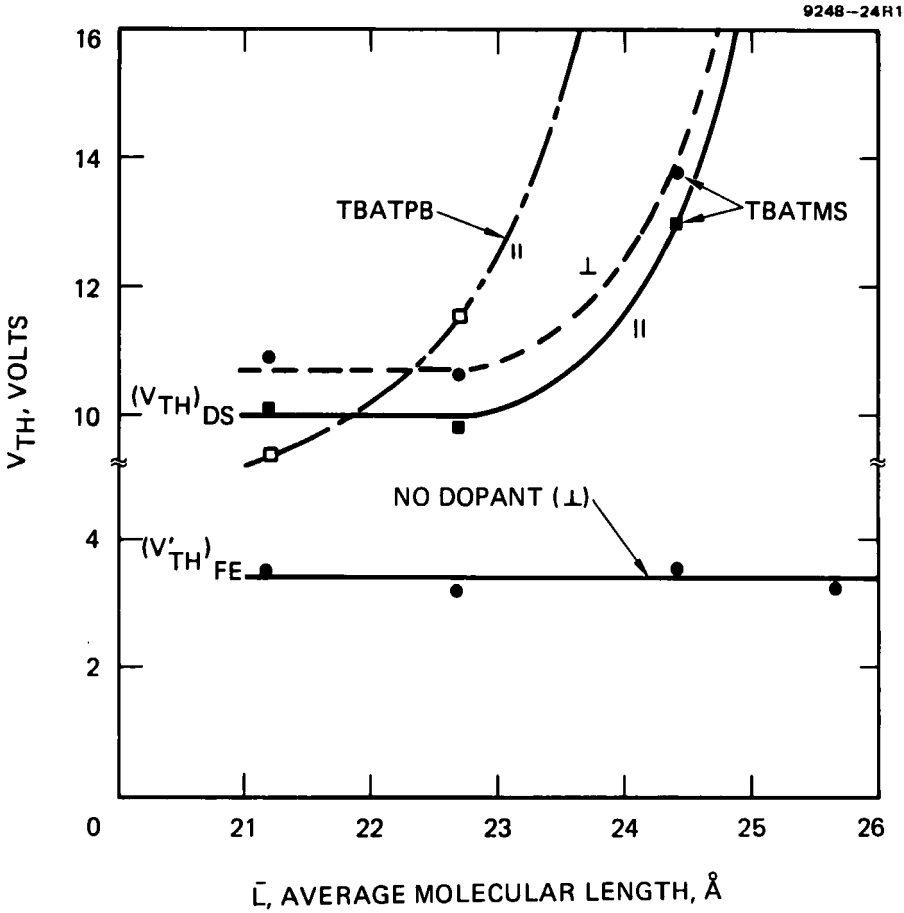

FIGURE 10 Threshold voltages at 25°C for field-effect transition (1 kHz) and dynamic scattering (10 Hz) as a function of $\bar{L}$ in *RO*-(C)*R'* mixtures.

TABLE IV

Bend elastic constant at 25°C

Mixture	$(V'_{th})_{FE}$	$\Delta\epsilon$	$k_{33} \times 10^{11}$, N
A	3.50	−1.34	1.47
C	3.20	−1.26	1.16
D	3.56	−1.24	1.41
E	3.23	−1.25	1.17

Downloaded by [Tomsk State University of Control Systems and Radio] at 03:12 23 February 2013

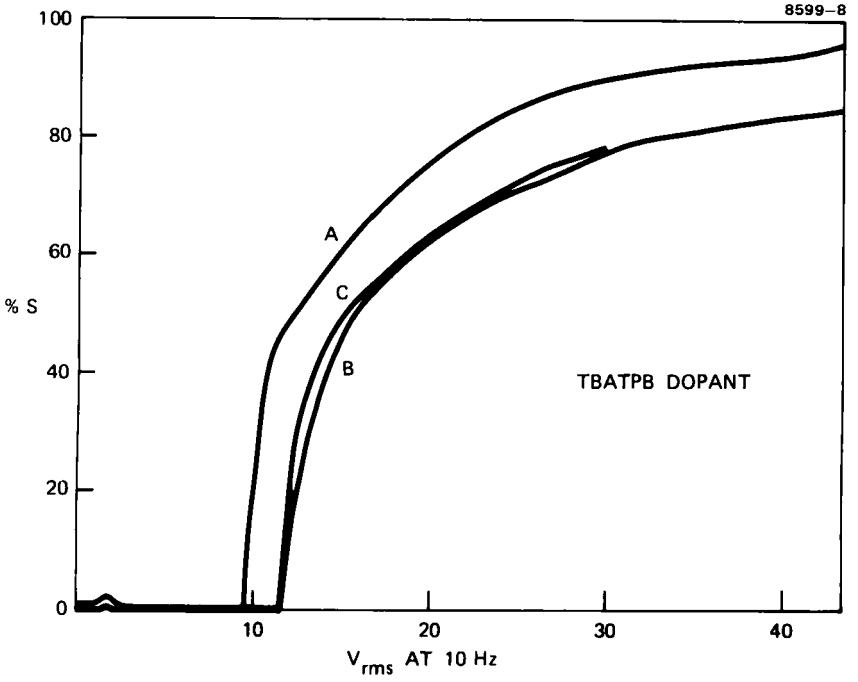

FIGURE 11 Dynamic scattering curves for mixtures A, B, and C containing TBATPB dopant. (22°C, 13-μm-thick cells surface-|| alignment). A: $\rho_\perp = 5.1 \times 10^9$ Ω-cm; B: $\rho_\perp = 6.1 \times 10^9$ Ω-cm; C: $\rho_\perp = 7.4 \times 10^9$ Ω-cm.

Dynamic scattering

Typical DS curves (where %S = 100 − %T) for mixtures A, B, and C are shown in Figure 11. These are run at low frequency (10 Hz) to minimize effects from the cut-off frequencies of these samples, which have relatively high resistivities due to the low solubility of the TBATPB dopant. The $(V_{th})_{DS}$ values from these curves are shown in Figure 10. In the other mixtures, TBATPB does not provide adequate conductivity for DS studies, and mixtures E, F, and G are not expected to show DS at 25°C anyway because their $\sigma_\parallel/\sigma_\perp$ ratios are less than 1.0. The TBATMS dopant is more soluble and gives better DS curves; the DS threshold voltage for mixtures A, C, and D are shown in Figure 10 for both surface-|| and surface-⊥ alignment. (These samples have resistivities of $\rho_\perp = 1.6 \times 10^9$, 1.8×10^9, and $4.9 = 10^9$ Ω-cm, respectively.) The general trend is that $(V_{th})_{DS}$ increases with $\bar{L}$ with either the TBATPB or the TBATMS dopant. These results are consistent with the conductivity anisotropy effects shown in Figures 5 through 7. Temperature effects on DS also correspond to the $\sigma_\parallel/\sigma_\perp$ changes. TBATMS doped mixture F shows high-

Downloaded by [Tomsk State University of Control Systems and Radio] at 03:12 23 February 2013

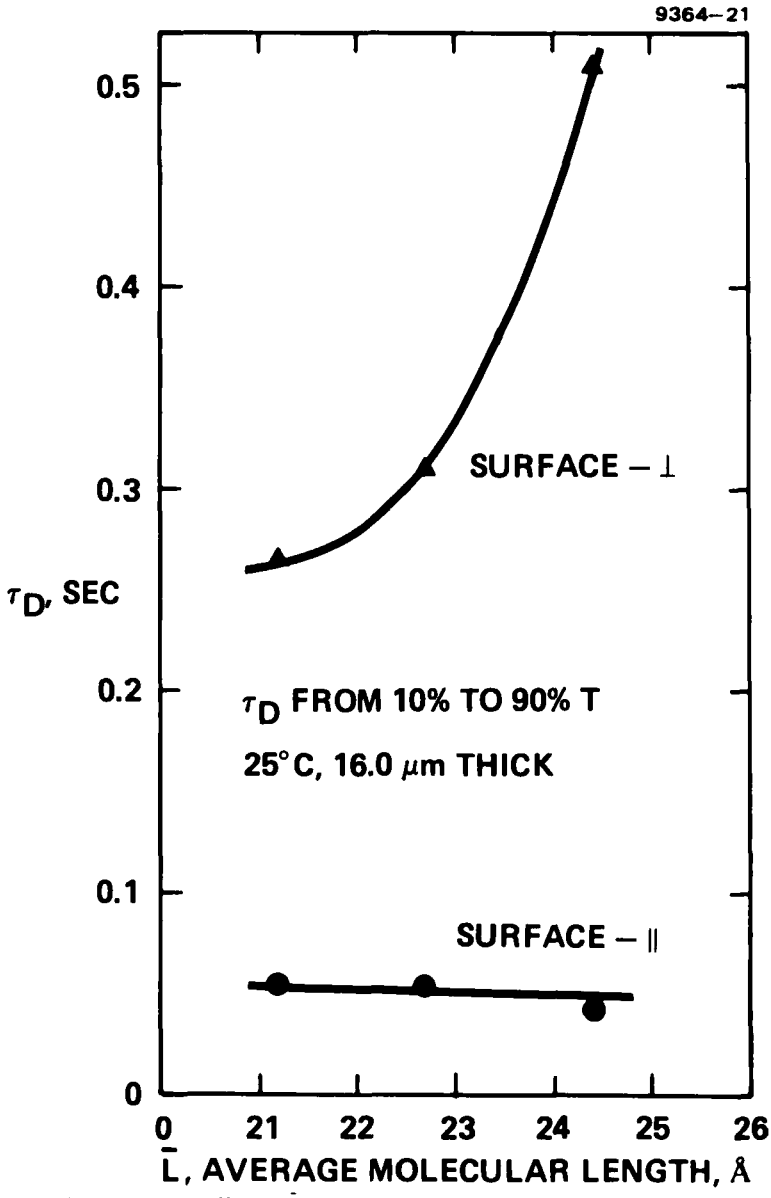

FIGURE 12 Effect of $\bar{L}$ on DS decay time in *RO*-(C)*R'* mixtures.

level scattering curves at higher temperatures (e.g., 60° C). Its $(V_{th})_{DS}$ value decreases sharply as temperature increases, going from an ill-defined 30 to 40 V value at room temperature, to ~20 V at 42° C, and down to 13.5 V at 53° C in surface-|| cells. Sample G does not show any DS below 35° C with either dopant, as expected since $\sigma_{\parallel}/\sigma_{\perp}$ is less than 1.0 in this temperature range.

Downloaded by [Tomsk State University of Control Systems and Radio] at 03:12 23 February 2013

The DS decay time (τ_D) of TBATMS-doped samples of mixtures A, C, and D are shown in Figure 12. For comparison, the decay times are corrected to 16.0 μm thickness, using a $16^2/l^2$ correction factor. The actual thickness between the optical flats are 15.43 μm for the surface-|| and 15.86 μm for the surface-$\perp$ cells. Although high voltages (50 V_{rms}) are applied to mixture D to obtain high scattering levels (10% T), secondary scattering is not observed with our relatively short periods of DS activation. The effect of $\bar{L}$ on τ_D is very similar to that observed in the *RO–R'* mixtures.[7] As $\bar{L}$ increases, τ_D for surface-|| cells decreases slightly, while τ_D for surface-$\perp$ cells increases substantially. However, all of these decay times are much faster than those of the corresponding phenyl benzoate mixtures. In the same $\bar{L}$ range, the τ_D's of the *RO–R'* mixture were about 375 msec for surface-|| and between 610 and 780 msec for surface-$\perp$ cells.

CONCLUSIONS

Studies of nematic mixtures of 4-alkoxyphenyl *trans*-4-alkylcyclohexanecarboxylates show that their viscosities, conductivity anisotropies, and DS threshold voltages are very strongly dependent on the average molecular length of the mixtures. As $\bar{L}$ increases, their viscosities increase exponentially and their cybotactic nematic character increases greatly. At 25° C, the short $\bar{L}$ cyclohexane ester mixtures have higher $\sigma_{\|}/\sigma_{\perp}$ values and much lower flow viscosities than do the comparable benzoate esters. The longer $\bar{L}$ cyclohexane ester mixtures have stronger cybotactic nematic characteristics and much lower $\sigma_{\|}/\sigma_{\perp}$ values (less than 1.0) and are just as viscous as the same length benzoate mixtures. The dielectric anisotropies of the cyclohexane esters also vary with $\bar{L}$, linearly becoming less negative as $\bar{L}$ increases. Their birefringences are nearly independent of $\bar{L}$. The solubility of organic salt dopants is low, and becomes worse as $\bar{L}$ increases. Comparisons with similar length *p*-alkoxyphenyl *p*-alkylbenzoate mixtures show that the short length cyclohexane ester mixtures have much more negative $\Delta\epsilon$, higher $\sigma_{\|}/\sigma_{\perp}$, lower DS at a given V/V_{th}, and much faster DS decay times in both surface-|| and surface-$\perp$ cells.

Acknowledgments

We are indebted to the Directorate of Chemical Sciences, Air Force Office of Scientific Research, Contract F49620-77-C-0017 for partial financial support of this research; to C. I. van Ast for assistance in liquid chromatography analyses; and to W. H. Smith, Jr., for assistance in DSC measurements.

References

1. D. Demus, H. J. Deutscher, F. Kuschel and H. Schubert, Bundes republic Deutschland Patentant 2429093 (1975).

Downloaded by [Tomsk State University of Control Systems and Radio] at 03:12 23 February 2013

2. R. Eidenschink, D. Erdmann, J. Krause and L. Pohl, *Angew. Chem.*, **89**, 103 (1977).
3. L. Pohl, R. Eidenschink, J. Krause and D. Erdmann, *Phys. Lett.*, **60A**, 421 (1977).
4. R. Eidenschink, D. Erdmann, J. Krause and L. Pohl, 7th International Liq. Cryst. Conf., Bordeaux, France, 1978 (Paper No. A04).
5. G. W. Gray and D. G. McDonnell, *Mol. Cryst. Liq. Cryst.*, **53**, 147 (1979).
6. Hp. Schad, G. Bauer and G. Meier, *J. Chem. Phys.*, **70**, 2770 (1979).
7. J. D. Margerum, J. E. Jensen and A. M. Lackner, Symposium on the Physics and Chemistry of Liquid Crystal Devices, San Jose, CA., Feb. 1979. (Paper I of this series; *Mol Cryst. Liq. Cryst.*, preceeding paper.)
8. J. D. Margerum, H. S. Lim, P. O. Braatz and A. M. Lackner, *Mol. Cryst. Liq. Cryst.*, **38**, 219 (1977).
9. L. J. Miller, J. Grinberg, G. D. Myer, D. S. Smythe and W. H. Smith, *Liquid Crystals and Ordered Fluids*, **3**, p. 513, J. E. Johnson and R. S. Porter, eds. (Plenum Pub. 1978).
10. J. D. Margerum, A. M. Lackner and H. S. Lim (Paper No. DP28), 7th International Liquid Crystal Conf., Bordeaux, France, July 1978.
11. F. Rondelez, *Solid State Comm.*, **11**, 1675 (1972).
12. A. Mircea-Roussel, L. Legar, F. Rondelez and W. H. DeJeu, *J. de Physique, Colloq.*, **C136**, 93 (1975).
13. G. Heppke and F. Schenider, *Z. Naturforsch.*, **309**, 316 (1975).
14. A. DeVries, *J. de Physique (Paris) Colloq.*, **C136**, 1 (1975).

Downloaded by [Tomsk State University of Control Systems and Radio] at 03:12 23 February 2013